

## Lasers in Manufacturing Conference 2021

# Experimental setup for determination of absorption coefficient of laser radiation in molten metals as a function of temperature and angle

Tjorben Bokelmann<sup>a\*</sup>, Marius Lammers<sup>a</sup>, Jörg Hermsdorf<sup>a</sup>, Sobhan Emadmostoufi<sup>b</sup>, Oleg Mokrov<sup>b</sup>, Rahul Sharma<sup>b</sup>, Uwe Reisgen<sup>b</sup>, Stefan Kaierle<sup>a</sup>

<sup>a</sup>Laser Zentrum Hannover e.V., Hollerithalle 8, 30419 Hannover, Germany

<sup>b</sup>Welding and Joining Institute RWTH Aachen University, Pontstraße 49, 52062 Aachen, Germany

---

### Abstract

For the process development of laser assisted double wire welding with nontransferred arc (LDNA), the simulation of the molten pool and its interaction with the laser radiation is of great importance. Therefore, an experimental setup for the determination of the temperature and angle dependent absorption coefficient of laser radiation in molten metals such as stainless steel will be presented. An Yb:YAG disc laser with 1030 nm is used as laser beam source. The stationary molten metal is inductively warmed and superheated by the laser beam with approximately 300-1000 W, whose radiation is shaped by homogenizing optics and ensures equal intensity when angle is adjusted.

Keywords: molten metal; absorption coefficient; laser beam; LDNA; temperature; angle

---

### 1. Introduction

Laser assisted double wire welding with nontransferred arc (LDNA) is a cladding process developed at Laser Zentrum Hannover e.V. and characterized by the spatial separation of the arc and laser beam, as shown in Figure 1 (Barroi et al., 2013; Barroi et al., 2014; Barroi et al., 2016). The arc burns between two wires, causing them to melt, impact the substrate surface in a droplet shape by gravity, and form a melt pool with the base material. By positioning the laser beam at the front of the melt pool, the material is pulled in the welding direction, so that a homogeneous temperature profile and a low degree of mixing of up to 5% are achieved over the transverse direction at deposition rates of up to 20 kg/hr. In order to gain a fundamental understanding of the physical sub-processes, the interaction of the laser beam with the melt pool is to be investigated in more detail.

For the usage in a CFX simulation model of the LDNA process, the absorption coefficient has to be determined. Therefore, an experimental setup is presented which the wire-shaped material is heated to a molten state and then heated with a laser beam. Through the temperature increase as a result of the supplied thermal energy of the laser, the absorption coefficient is to be determined.

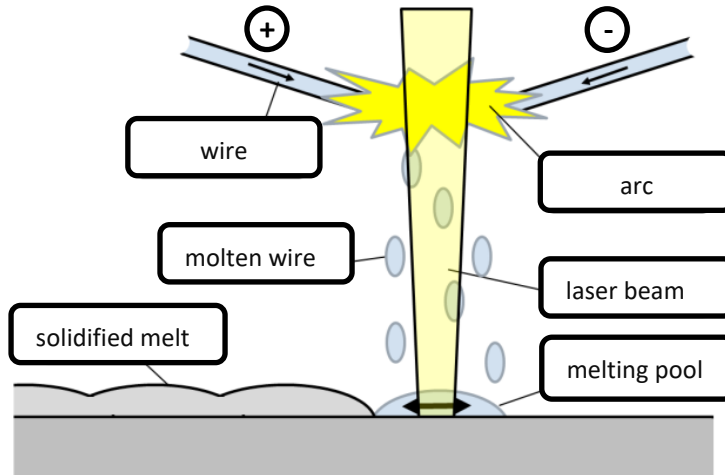


Fig. 1. Principle of the LDNA process.

## 2. State of the art

While the measurement methods of (Hsia and Richmond, 1976) for the determination of the absorption coefficient are based on reflection, (Hipp, 2020) uses a thermal camera for the angle-dependent determination of the coupling of laser radiation onto a translationally moving substrate made of stainless steel (1.4301), as shown in figure 2. The experimental setup allows measurements for angles between  $0^\circ$  and  $86^\circ$  with respect to the vertical axis in normal atmosphere and takes the heat distribution in the component due to the angle-dependent intensity into account. A collimated laser beam with 50 mm focal length from a fiber laser with 1070 nm heats the thermally insulated substrate and the temperature is measured in four areas located outside the heat interaction zone with the aid of the thermal camera, as the heat distribution is determined by matching the experimentally identified time-temperature curves with the numerical model for heat conduction. In the case of a match with the simulative model, the degree of coupling is determined directly from the time-temperature curve.

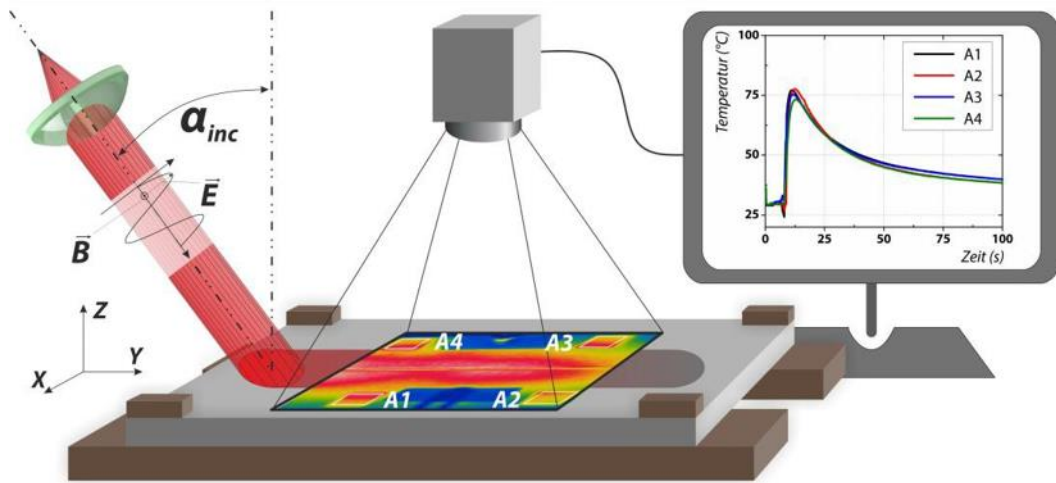


Fig. 2. Translatory experimental setup for determination of absorption coefficient of laser radiation (Hipp, 2020).

(Gipperich et al., 2020), on the other hand, follow the approach of isobaric heating of the sample with a continuous laser beam that is subsequently dropped into a container with water as in Figure 3. By measuring the temperature change and heat capacities of the sample and water, the absorption coefficient is determined. The simultaneous use of a pulsed laser beam increases the absorption up to 20%. According to this method, the absorption coefficient  $\alpha$  is calculated by following equation:

$$\alpha = \frac{E}{P \cdot t} \text{ and} \quad (1)$$

$$E = m \cdot c (T - T_{0,L}) + m c (T - T_{0,S}). \quad (2)$$

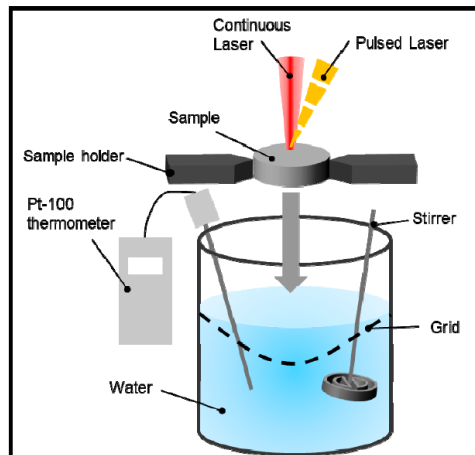


Fig. 3. Calometric experimental setup for determination of absorption coefficient of laser radiation (Gipperich et al., 2020).

### 3. Materials and Methods

While the measurement methods of (Hipp, 2020) for determining the absorption coefficient are based on time-temperature curves using a thermal camera, (Gipperich et al., 2020) use the principle of measuring the temperature change using the heat capacities of mild steel and water. Both determine the degree of coupling of laser radiation to metals in the solid state. In the current paper, however, an experimental setup is presented that is used to determine the degree of coupling into molten metals.

Figure 4 shows this experimental setup, which is based on the two forms of energy input by induction and laser radiation. With the aid of an induction generator with an output power of up to 3 kW, wire-shaped stainless steel (1.4430) is heated in a tungsten crucible in a normal atmosphere at 1013 mbar from 20 °C to above the solidus temperature of approx. 1410 °C, so that a superheated melt is produced in the steady state. Subsequently, a defocused laser beam is used to heat the melt on the surface until the melt heats up by approximately 50 °C and a steady state is again achieved. The degree of coupling is to be determined from the thermal energy supplied by the laser beam during this period and the temperature increase.

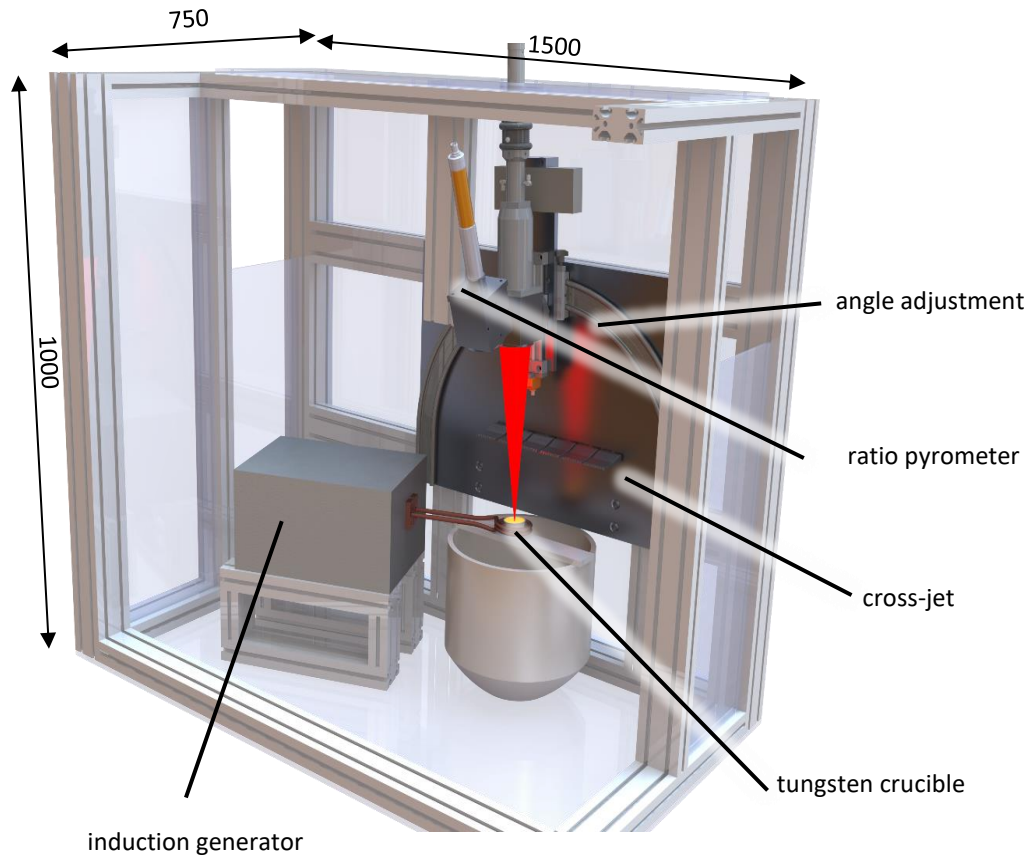


Fig. 4. Experimental setup for determination of absorption coefficient of laser radiation of molten metal.

For this purpose, the tungsten crucible is located on a 20 mm plate made of fireclay that is permanently temperature-resistant up to 1300 °C and is used in stoves. Radially, the distance between the crucible and the inside of the coil is 2.5 mm. The linear thermal expansion is temperature-dependent and is calculated according to

$$\Delta L = L_0 \int_{T_1}^{T_2} \alpha(T) dT. \quad (3)$$

To estimate the thermal expansion of the crucible, the linear coefficient of thermal expansion for tungsten of  $4 \cdot 10^{-6} \cdot K^{-1}$  is assumed, so that from 20 °C to 1520 °C the following thermal expansion results

$$\Delta L = 55 \text{ mm} \cdot 4 \cdot 10^{-6} \cdot \frac{1}{K} \cdot (1520 - 20) K = 0,5 \text{ mm}. \quad (4)$$

The test environment of the crucible is filled with argon 4.6 and, during heating, is also flooded with argon 4.6 using a cross-jet approx. 100 mm above the top edge of the crucible in order to dissipate the radiant heat in the direction of the opposite exhaust and to protect the optics. To ensure an inert environment, an oxygen meter is used to measure the oxygen content in the process environment at four points radially to the coil and at four points above the crucible.

The laser beam source is a Yb:YAG disk laser with a fiber core diameter of 600 µm, up to 16 kW output power and 1030 nm emission wavelength. The laser beam is guided through a collimator with 200 mm focal length and a focusing lens with 150 mm focal length. The distance between the focusing lens and the top edge of the crucible can be adjusted between 200 mm and 400 mm via a linear stage, while the angle between the laser beam and the crucible can be practically set between 0 ° and 80 ° via a round rail. Since the effective area of the laser beam on the surface of the molten metal in the crucible changes due to the angle adjustment, homogenizing optics will be used in further investigations so that the intensity remains constant by adjusting the rectangular beam profile. The defocused laser beam as shown in Figure 5 is used to supply the thermal energy over a larger area and to heat the molten metal more homogeneously. The diameter of the defocused laser beam is approximately 22 mm in the plane on the top edge of the crucible at an angular setting of 6.4 ° to the vertical axis at a distance of 220 mm.

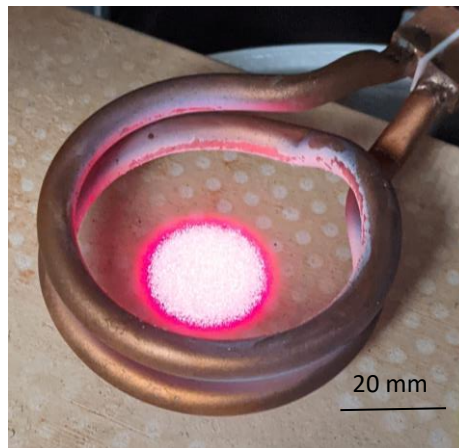


Fig. 5. Defocused laser beam with 23 mm diameter for melting stainless steel in a tungsten crucible.

The temperature of the stainless steel in the crucible is measured with a Metis M322 ratio pyrometer from Sensortherm with a spot diameter of 2.3 mm at a distance of 400 mm from the surface of the crucible and allows measurement without knowledge of the emissivity of the material under investigation. Furthermore, the temperature of the stainless steel, whose chemical composition is given in Table 1, is determined over a large area using Infratec's Image IR® 8300 infrared thermal camera by varying the displayed temperature with that of the pyrometer by adjusting the emissivity. A listing of the devices with their characteristics used for this experimental setup is given in Table 2.

Table 1. Chemical deposition of material determined with an EDX-scan at 18 spots and with standard deviation P = 99 %.

Material (DIN 8556)	Material No.	Fe [wt %]	Cr [wt %]	Ni [wt %]	Mo [wt %]	Mn [wt %]	Si [wt %]	C [wt %]
SG X 2 CrNiMo 19 12	1.4430	64,9 ± 1,1	18,3 ± 0,5	11,0 ± 1,1	2,8 ± 0,5	1,8 ± 0,4	0,8 ± 0,3	0,18 ± 0,10

Table 2. Devices

Device	Producer	Model	Characteristic	Value
Crucible	SITUS Technicals	Tungsten > 99.9 %	External diameter/ Wall thickness / Height	55 mm / 2 mm / 28 mm
Disc laser	TRUMPF	TrueDisc16002	Output power	320-16.000 W
			Emission wavelength	1.030 nm
			Beam quality	16 mm · mrad
Optical fiber			Fiber diameter	600 µm
Collimation lens	Thorlabs		Collimation length	200 mm
Focus lens	TRUMPF		Focus length	150 mm
Ratio pyrometer	Sensortherm	Metis M322	Wavelength	1.45-1.65 µm / 1.65-1.85 µm
Thermal camera	Infratec	Image IR® 8300	Frames per second	300 Hz

#### 4. Results

When the induction generator is turned on, the tungsten crucible initially starts to couple the induction voltage faster than the stainless steel, so that the crucible heats up and glows. The coupling is initially 60 % of the output power, i.e. approx. 1800 W, but increases to 70 % with temperature. From approx. 600 °C, the measuring range of the ratio pyrometer begins and shows the temperature curve as in Fig. 6. Since the radiant heat also increases with the temperature, the temperature approaches a limit value asymptotically. This is about 970 °C, so that the heating due to the induction voltage is exactly as great as the heat emitted, which is characterized by heat conduction to the refractory brick, convection due to the gas flow of the cross-jet and the water-cooled induction coil, as well as the radiant heat, as can be seen in Figure 7. The radiant heat is calculated with a crucible surface area of 16,200 mm<sup>2</sup>, an emissivity of unoxidized steel of 0.61 at 1000 °C and a temperature of 970 °C according to

$$P = A \sigma \epsilon T^4 = 16.200 \text{ mm}^2 \cdot 6,12 \cdot 10^{-8} \text{ W} \frac{1}{\text{m}^2 \text{K}^4} 0,61 (970 \text{ K} + 273,15 \text{ K})^4 = 1444,4 \text{ W}. \quad (3)$$

As more oxygen from the environment enters the process zone during the process due to convection from the argon flow of the cross-jet, oxidation of the stainless steel and tungsten occurs. The emissivity of the oxidized stainless steel is therefore 0.96-0.98, resulting in the following radiant heat

$$P = A \sigma \epsilon T^4 = 16.200 \text{ mm}^2 \cdot 6,12 \cdot 10^{-8} \text{ W} \frac{1}{\text{m}^2 \text{K}^4} \cdot 0,98 (970 \text{ K} + 273,15 \text{ K})^4 = 2320,5 \text{ W}. \quad (4)$$

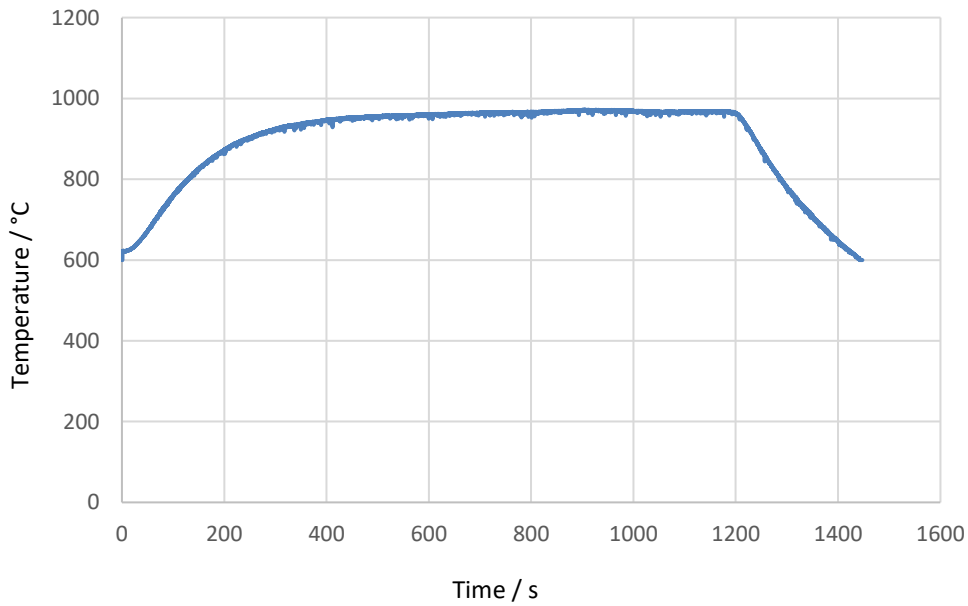


Fig. 6. Inductively warmed stainless steel specimen in a tungsten crucible.

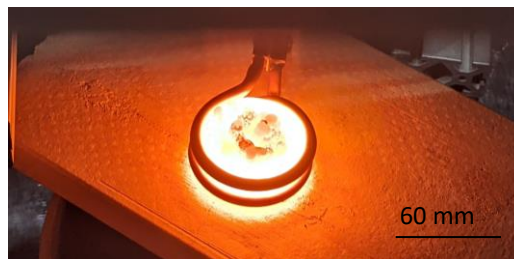


Fig. 7. Inductively heated stainless steel in a tungsten crucible at 970 °C.

Since the inductor power of 3 kW is not sufficient for melting, the defocused laser beam was additionally directed onto the stainless steel in the crucible when 900 °C was reached. Figure 8 shows the temperature profile over time for laser output powers from 320 W to 700 W. From these experiments, it can be seen that

once 900 °C is reached, the inductive heating causes the temperature to rise abruptly, even at the lowest power of 300 W. However, this method is not practicable for future experiments to set the temperature specifically. This challenge increases accordingly with higher power levels. Furthermore, it has been shown that the inert gas atmosphere present is not sufficient to prevent oxidation of the stainless steel. This can be seen from the longer irradiation time of approx. 5 min at a laser power of 700 W. The temperature only stagnates at approx. 1650 °C due to the melting process and does not already reach the solidus temperature at 1410 °C. At this point the material enters the two-phase region for melting and at the liquidus temperature the melting process is completed. An overheating of the melt ensures a steady state point.

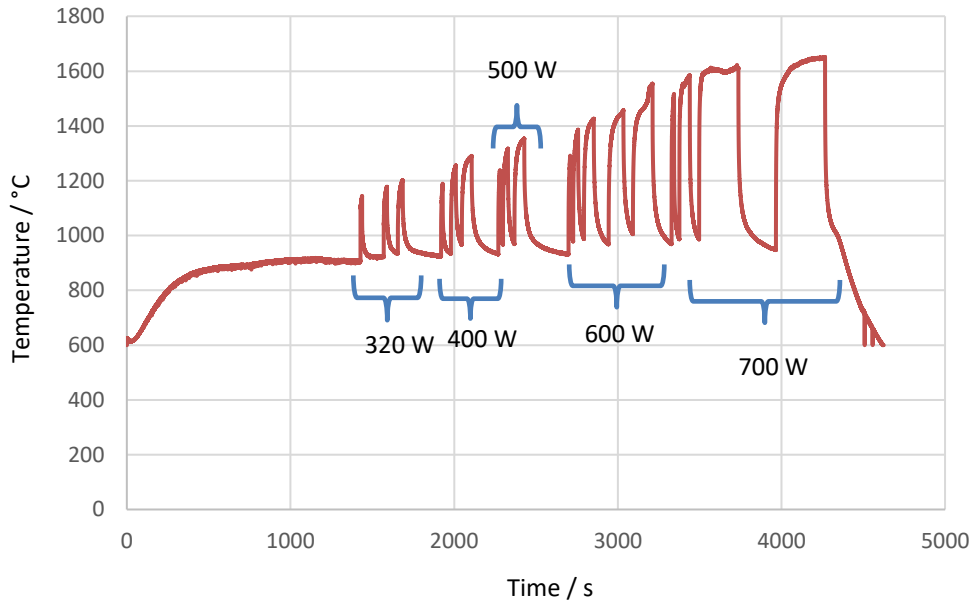


Fig. 8. Inductively heated stainless steel in a tungsten crucible at 900 °C and additional heating with laser beam.

## 5. Conclusions

This paper presents an experimental setup for determining the angle- and temperature-dependent degree of coupling of laser radiation into molten metal using stainless steel (1.4430). The method is based on a combination of thermographic and calorimetric measurement of the temperature and thus neither measures the reflection nor requires knowledge of the emissivity of the material under investigation.

When inductively heating the wire-shaped stainless steel in a tungsten crucible, only a magnetic coupling of 70 % could be achieved with an output power of 3 kW, so that the temperature asymptotically approaches a value of approx. 970 °C. Additional heating of the material with a defocused laser beam proved impractical due to the high temperature jump of several hundred degrees Celsius, even at low powers. Furthermore, despite purging the process zone with argon before the start of the process and additionally using a cross-jet during the test, a sufficient inert gas atmosphere could not be guaranteed. As a result, both the stainless steel and the tungsten crucible oxidize, which is why the melting process does not start until 1650 °C during heating with the laser beam.



In the next step, therefore, an induction coil for an induction generator with an output power of up to 8 kW is used to bring the material into the molten state in a controlled and homogeneous manner and to achieve steady-state equilibrium. Afterwards, a laser beam is directed onto the surface of the melt and the absorption coefficient is measured. Furthermore, the gas flow is optimized to achieve a sufficient protective gas atmosphere of approx. 500 ppm oxygen in the process.

## Acknowledgements

A special gratitude is addressed to the German Research Foundation (DFG), which funded this basis research project with the number 423140171.

## References

- Barroi, A., Hermsdorf, J., Prank, U., Kaierle, S., 2013. A novel approach for high deposition rate cladding with minimal dilution with an arc – Laser process combination, *Physics Procedia* 41. Science Direct, pp 249-254. DOI: <http://dx.doi.org/10.1016/j.phpro.2013.03.076>.
- Barroi, A., Ameila, J., Hermsdorf, J., Kaierle, S., Wesling, V., 2014. Influence of the Laser and its Scan Width in the LDNA Surfacing Process, *Physics Procedia* 56, pp. 204-210. DOI: 10.1016/j.phpro.2014.08.164.
- Barroi, A., Zimmermann, F., Hermsdorf, J., Kaierle, S., Wesling, V., Overmeyer, L., 2016. Evaluation of the laser assisted double wire with nontransferred arc surfacing process for cladding, *Journal of Laser Applications* 28 (2), pp. 1-4. DOI: <http://dx.doi.org/10.2351/1.4944001>.
- Gipperich, M., Riepe, J., Arntz, K., Bergs, T., 2020. Pulsed Laser Influence on Temperature Distribution during Dual Beam Laser Metal Deposition, *MDPI metals* 766 (2), pp. 1-11. DOI: :10.3390/met10060766.
- Hipp, D., 2020. Einkopplung von Laserstrahlung unter Prozessbedingungen der Materialbearbeitung – Entwicklung einer Bestimmungsmethodik und Ergebnisse, Technical University Dresden, Germany, PhD thesis. Available at <https://core.ac.uk/download/pdf/353950985.pdf>.